Redox Biology 67 (2023) 102902

Contents lists available at ScienceDirect

Redox Biology

journal homepage: www.elsevier.com/locate/redox

The Arabidopsis thioredoxin TRXh5regulates the S-nitrosylation pattern of the TIRK receptor being both proteins essential in the modulation of defences to *Tetranychus urticae*

Ana Arnaiz [a,1], Maria C. Romero-Puertas [b,**], M. Estrella Santamaria [a], Irene Rosa-Diaz [a], Vicent Arbona [c], Alfonso Muñoz [d], Vojislava Grbic [e], Pablo González-Melendi [a,f], M. Mar Castellano [a], Luisa Maria Sandalio [b], Manuel Martinez [a,f], Isabel Diaz [a,f,*]

[a] Centro de Biotecnología y Genómica de Plantas (CBGP), Universidad Politécnica de Madrid (UPM)-Instituto Nacional de Investigación y Tecnología Agraria y Alimentaria/CSIC, Campus de Montegancedo, 20223, Madrid, Spain
[b] Department of Biochemistry and Molecular and Cellular Biology of Plants, Estación Experimental del Zaidín, CSIC, Granada, Spain
[c] Departament de Biologia, Bioquímica i Ciències Naturals, Universitat Jaume I, E-12071, Castelló de la Plana, Spain
[d] Departamento de Sistemas y Recursos Naturales. Escuela Técnica Superior de Ingeniería de Montes, Forestal y del Medio Natural, UPM, Madrid, Spain
[e] Department of Biology, University of Western Ontario, N6A 5BT, London, Ontario, Canada
[f] Departamento de Biotecnología-Biología Vegetal, Escuela Técnica Superior de Ingeniería Agronómica, Alimentaria y de Biosistemas, UPM, Madrid, Spain

A B S T R A C T

The interaction between plants and phytophagous arthropods encompasses a complex network of molecules, signals, and pathways to overcome defences generated by each interacting organism. Although most of the elements and modulators involved in this interplay are still unidentified, plant redox homeostasis and signalling are essential for the establishment of defence responses. Here, focusing on the response of *Arabidopsis thaliana* to the spider mite *Tetranychus urticae,* we demonstrate the involvement in plant defence of the thioredoxin TRXh5, a small redox protein whose expression is induced by mite infestation. TRXh5 is localized in the cell membrane system and cytoplasm and is associated with alterations in the content of reactive oxygen and nitrogen species. Protein S-nitrosylation signal in *TRXh5* over-expression lines is decreased and alteration in *TRXh5* level produces changes in the JA/SA hormonal crosstalk of infested plants. Moreover, TRXh5 interacts and likely regulates the redox state of an uncharacterized receptor-like kinase, named THIOREDOXIN INTERACTING RECEPTOR KINASE (TIRK), also induced by mite herbivory. Feeding bioassays performed with*TRXh5* over-expression plants result in lower leaf damage and reduced egg accumulation after *T. urticae* infestation than in wild-type (WT) plants. In contrast, mites cause a more severe injury in *trxh5* mutant lines where a greater number of eggs accumulates. Likewise, analysis of *TIRK*-gain and -loss-of-function lines demonstrate the defence role of this receptor in Arabidopsis against *T. urticae*. Altogether, our findings demonstrate the interaction between TRXh5 and TIRK and highlight the importance of TRXh5 and TIRK in the establishment of effective Arabidopsis defences against spider mite herbivory.

1. Introduction

Thioredoxins (TRXs) are ubiquitous oxidoreductases responsible for transient and reversible redox-based posttranslational modifications [1]. These modifications involve the redox state of structural or catalytic protein cysteines and comprise oxidative and/or nitrosative modifications of cysteine thiols, such as reduction of S–S bonds and S-denitrosylation of –SNO groups [2]. Arabidopsis encodes 20 conventional TRXs, eight of them belonging to the TRXh family, mainly located in the cytosol [3]. These proteins are highly versatile, as they can modulate a broad range of metabolic processes and responses of plants to biotic and abiotic stresses [4]. Whereas their role in plant immunity has been widely explored in response to pathogens [5,6], the participation of TRXs in response to herbivores has been poorly addressed. Nevertheless, as in the plant-pathogen interaction, reactive oxygen and nitrogen species (ROS/RNS) are key players for the redox homeostasis taking part in plant defences to phytophagous species [7,8].

* Corresponding author. Centro de Biotecnología y Genómica de Plantas (CBGP), Universidad Politécnica de Madrid (UPM)-Instituto Nacional de Investigación y Tecnología Agraria y Alimentaria/CSIC, Campus de Montegancedo, 20223, Madrid, Spain.
** Corresponding author.
E-mail addresses: a.arnaiz@upm.es (A. Arnaiz), maria.romero@eez.csic.es (M.C. Romero-Puertas), me.santamaria@upm.es (M.E. Santamaria), i.rosa@upm.es (I. Rosa-Diaz), vicente.arbona@camn.uji.es (V. Arbona), alfonso.munozg@upm.es (A. Muñoz), vgrbic@uwo.ca (V. Grbic), pablo.melendi@upm.es (P. González-Melendi), castellano.mar@inia.csic.es (M. Mar Castellano), luisamaria.sandalio@eez.csic.es (L.M. Sandalio), m.martinez@upm.es (M. Martinez), i.diaz@upm.es (I. Diaz).
[1] Current address: Universidad Politécnica de Madrid, Madrid, Spain.

https://doi.org/10.1016/j.redox.2023.102902
Received 27 July 2023; Received in revised form 8 September 2023; Accepted 21 September 2023
Available online 27 September 2023

Abbreviations

BiFC	Bimolecular Fluorescence Complementation
CoIP	CoImmunoprecipitation
DAB	3,3′-diaminobenzidine
DAMPs	Damage-Associated Molecular Patterns
GFP	Green Florescent Protein
HAMPs	Herbivory-Associated Molecular Patterns
JA	Jasmonic Acid
JA-Ile	JA-Isoleucine
OPDA	12-OxophytoDienoic Acid
PTMs	PostTranslational Modifications
RLK	Receptor-Like Kinase
RNS	Reactive Nitrogen Species
ROS	Reactive Oxygen Species
RT-qPCR	Quantitative Real Time PCR
SA	Salicylic Acid
TRX	Thioredoxin

The plant response to herbivores is initiated when specific receptors, mainly receptor-like kinases (RLK), detect either Herbivore-Associated Molecular Patterns (HAMPs) or Damage-Associated Molecular Patterns (DAMPs). Plants discriminate between herbivores to counteract specific threats more accurately. Commonly, the first steps in the adjustment of the defence network begin with a membrane potential depolarization followed by changes in intracellular Ca^{2+} amount, ROS and RNS generation, and activation of specific protein kinases. Therefore, signalling networks are modified leading to the activation of transcription factors and the regulation of phytohormone synthesis, to finally culminate in the induction of specific herbivore-responsive genes [9,10]. In this context, various studies have increased the understanding of how Arabidopsis plants specifically recognize and signal the attack of the two-spotted spider mite *Tetranychus urticae* Koch (Acari: Tetranychidae). Most of these studies were based on a transcriptomic comparison of responses between Blanes-2 (Bla-2) and Kondara (Kon) Arabidopsis accessions, identified as the most resistant and the most susceptible to *T. urticae,* among 26 tested Arabidopsis accessions [11]. Hundreds of genes responded similarly to *T. urticae* attack and dozens of them were induced at higher levels in Bla-2 than in Kon. Several of these genes, e.g. *AtKTI4*, *MATI*, and *PP2-A5*, have been characterized and their requirement for Arabidopsis resistance to mite herbivory has been demonstrated [12–14]. Additionally, it was shown the role of an Arabidopsis Ser/Thr phosphatase type 2C, AP2C1 and the MAPKinases MPKKK17 and MPKKK21 in the regulation of the signalling pathways triggered by the mite [15,16]. Recently, it has been highlighted the important defence role of indole glucosinolates and the hydroxinitrile lyase AtHNL, whose levels increased upon mite infestation [17,18].

Regarding redox homeostasis, the relationship between ROS-metabolizing systems and Arabidopsis-induced responses triggered by mites was established using four ROS-related genes differentially induced in Bla-2 and Kon after mite attack. These genes encode proteins involved in hydrogen peroxide (H_2O_2) balance and ascorbate degradation. In addition to their effects on ROS metabolism, genetic manipulation of these genes led to an alteration of jasmonic acid (JA) and salicylic acid (SA) signalling pathways and consequently, to plant defence against spider mites [9,19]. One of the genes induced by mite feeding with higher expression levels in Bla-2 relative to Kon is the thioredoxin h5 (*TRXh5)*. This *TRX* gene has previously been associated with the regulation of SA-related immune gene expression by NPR1 after pathogen challenge [20]. In the cytoplasm, NPR1 forms a high molecular weight oligomer through disulphide bonds between conserved cysteine residues, promoted by an S-nitrosylation of Cys156. Upon activation of SA signalling, TRXh5 facilitates the monomerization of NPR1 by reducing disulphide bonds and acting as an S–NO reductase. NPR1 monomers are then translocated into the nucleus where they activate SA-responsive immune genes [21]. In addition, TRXh5 acts as a guardee of the NB-LRR resistance protein LOV1, preventing the cell death-inducing activity of this protein in response to biotrophic pathogens [22]. The necrotrophic fungus *Cochliobolus victoriae* takes advantage of this system by secreting a toxin, victorin, that binds to the Cys39 of TRXh5 [23]. This interaction inhibits TRXh5 activity and triggers LOV1-dependent programmed cell death that the fungus exploits as it feeds on dead tissue. TRX proteins have been also associated with protein folding, acting as molecular chaperones alone or synergistically with HSP chaperones to prevent cellular damage [24]. These findings highlight the importance of TRX activity in the regulation of redox-based posttranslational modifications of selective immune signalling proteins. In addition, they underline the significance of TRXh5 protein interactions in different physiological processes.

Here, we examine the role of TRXh5 in the plant response to mite attack. Multiple interactions between TRXh5 with other proteins support its role in shaping the Arabidopsis response to *T. urticae* herbivory. One of the interacting proteins is the THIOREDOXIN INTERACTING RECEPTOR KINASE (TIRK), a RLK transmembrane receptor whose expression is induced by mite infestation. Functional assays have established the requirement of TRXh5 and TIRK for the proper Arabidopsis response to mites, and demonstrated the importance of both proteins, whose interaction is crucial in the early establishment of effective Arabidopsis defence responses against spider mite herbivory. TRX5 modulates the S-nitrosylation of TIRK which could affect mite perception and/or triggering of the transduction pathway to finally lead defence responses.

2. Materials and methods

2.1. Plant material and growth conditions

A. thaliana Col-0, Kondara, and Bla-2 accessions (Nottingham Arabidopsis Seed Collection) were used to validate RNAseq data. For further experiments, Col-0 has been as background (WT and mutant lines). *A. thaliana* T-DNA mutants (SALK_113268C, SALK_144259, SALK_107466C, and SAIL_669_G08, referred to as *trxh5_1*, *trxh5_2*, *tirk_1* and *tirk_2*, respectively) were obtained from the Arabidopsis Biological Resource Centre, through the European Arabidopsis Stock Centre. For soil growth, a mixture of peat moss and vermiculite (2:1) was used. Sterilized *seeds were stratified* in the dark at *4 °C* for 5 d. Plants were grown in growth chambers (Sanyo MLR-351-H) under controlled conditions (23 °C ± 1 °C, >70% relative humidity, and a 16 h/8 h day/night photoperiod).

To generate over-expression lines, *TRXh5* and *TIRK* cDNAs were cloned into pGWB2 (CaMV35S, no tag) and pGWB5 (CaMV35S, C-sGFP) Gateway binary vectors [25], using specific primers included in Table S1. The *TIRK* full-length cDNA clone was developed by the plant genome project of the RIKEN Genomic Sciences Center [26,27]. Recombinant plasmids were introduced into *A. thaliana* Col-0 plants using *Agrobacterium* floral dip transformation [28]. Shoots were regenerated on a selective medium containing hygromycin (40 mg l^{-1}) and plants were self-fertilized twice to identify and select homozygous lines. Homozygous plants with a single copy insertion and the highest transgene expression levels coming from different transformation events were selected for further experiments.

2.2. Spider mite maintenance

A colony of *T. urticae*, London strain (Acari: Tetranychidae), provided by Dr. Miodrag Grbic (UWO, Canada), was reared on beans (*Phaseolus vulgaris*) and kept in growth chambers (Sanyo MLR-351-H, Sanyo, Japan) at 25 °C ± 1 °C, >70% relative humidity and a 16 h/8 h day/night photoperiod.

2.3. Nucleic acid analysis

The presence and homozygous status of the T-DNA insertion lines were validated by conventional PCR (BioRad) using specific primers designed through the Salk Institute website. Primer sequences are indicated in Table S1. The genomic DNA used for conventional PCR was isolated from Arabidopsis T-DNA insertion and WT lines basically as described [29].

RT-qPCR was used to validate the microarray results, to analyse the gene expression in different Arabidopsis tissues, to determine and characterize the gene expression in the transgenic lines, and to study the expression of other genes. For microarray validation, 3-week-old rosettes from Col-0, Bla-2, and Kon were collected at different time points (1, 3, 6, 12, and 24 h) of spider mite infestation, frozen in liquid N_2 stored at −80 °C until used for RNA isolation. For tissue expression, Col-0 seeds, siliques, roots, flowers, stem leaves, and rosettes of 1- to 3-week-old were sampled and stored at −80°C. To study the expression of *TRXh* and *TIRK* genes, 3-week-old rosettes of transgenic and WT were infested with 20 mite female adults for 6 and 24 h and then collected and stored at −80 °C until RNA isolation. Total RNA was extracted by the phenol/chloroform method, followed by precipitation with 8 M LiCl [30]. Complementary DNAs (cDNAs) were synthesized from 2 μg of RNA using the Revert Aid™ H Minus First Strand cDNA Synthesis Kit (Fermentas) following the manufacturer's instructions. The RT-qPCR conditions used were 40 cycles with 15 s at 95 °C, 1 min at 60 °C and 5 s at 65 °C using LightCycler® 480 SYBR® Green I Master (Roche). Quantitative real time PCR (RT-qPCR) was performed for three samples coming from three independent experiments as previously described [12] using a SYBR Green Detection System (Roche) and the LightCycler®480 Software release 1.5.0 SP4 (Roche). Ubiquitin was used as the housekeeping gene for Arabidopsis. mRNA quantification was expressed as relative expression levels (2^{-dCt}) or fold change (2^{-ddct}) [31]. Primer sequences are indicated in Table S1.

2.4. In silico analyses of TRXh5 interactors

The BIOGRID database [32] was mined to find experimentally validated TRXh5 interactors. Enrichment analyses for GO Biological Processes were performed with the Bonferroni step-down test using the ClueGO package [33] in Cytoscape [34].

2.5. Subcellular location

To analyse the subcellular localization of the TRXh5 and TIRK proteins, the corresponding cDNAs were cloned in frame with the *GFP* reporter gene, encoding the Green Fluorescent Protein, as described above. In addition, the Red Fluorescent Protein (RFP)-HDEL was used as a control of endoplasmic reticulum location [35]. Transient transformation of onion (*Allium cepa*) epidermal cells was performed by particle bombardment with a biolistic helium gun device (DuPont PDS-1000; BioRad) as described [36]. Fluorescent images were acquired after 24 h of incubation at 22 °C in the dark, using a Leica TCS-SP8 confocal microscope. *GFP and RFP signals were acquired sequentially using the following settings: GFP, excitation* 488 nm *and emission 492*–573 nm*; RFP, excitation* 561 nm*, emission 564*–641 nm.

For *Nicotiana benthamiana* agroinfiltration, the *Agrobacterium* strain C58CI RifR (*GV3101*) carrying the constructs 35S::TRX5-GFP or 35S::TIRK-GFP (pGWB5) was co-incubated with the construct 35S::P19 (pBIN61) that carries the silencing suppressor P19 to a final optical density of 0.3 as described [13]. Fluorescent images were acquired 3 d post-infiltration, using a Leica TCS-SP8 confocal microscope. *GFP and chlorophyll autofluorescence signals were acquired sequentially using the following settings: GFP, excitation* 488 nm *and emission 492*–573 nm*; chlorophyll, excitation* 633 nm*, emission 692*–736 nm.

2.6. Immunoprecipitation analysis

Immunoprecipitation assays were carried out as described by Ref. [37] *with minor modifications. Briefly, N. benthamiana leaves were agro-infiltrated with the* 35S::TRXh5-GFP construct (pGWB5) and/or 35S::TIRK fused in frame to the HA epitope (pGWB14) *and harvested after 3 d. 1.2 g of each sample were ground in liquid N2 and incubated in 4 ml g-1 of extraction buffer (*50 mM *Tris-HCl* pH *7.5,* 150 mM *NaCl, 5% (v/v) glycerol, 0.1% (v/v) Nonidet P40,* 5 mM *DTT, 2% (w/v) poly-(-vinylpolypyrrolidone) and protease inhibitors (Roche)) with end-over-end shaking for* 15 min*. After centrifugation at 2500 g for* 20 min*, supernatants were centrifuged at 20,000 g for* 30 min*, collected and considered crude extracts. The protein concentration was measured by the Bradford method* [38]*. Co-immunoprecipitation mixtures were made containing the same amounts of total protein in the same volume. These mixtures were incubated with constant rotation for 1.5 h with* 30 μl *of anti-GFP agarose beads (ChromoTek), previously blocked to avoid unspecific binding with 1 mg ml-1 BSA in extraction buffer without poly-(vinylpolypyrrolidone). Subsequently, the beads were collected by centrifugation, washed 5 times with* 1 ml *of the extraction buffer without poly-(vinylpolypyrrolidone), and eluted with* 100 μl *of* 50 mM *glycine-HCl (*pH *3),* 150 mM *NaCl, 0.1% (v/v) Triton X-100 at room temperature for* 5 min*. After elution, the fractions were neutralized using* 10 μl *of 1 M Tris-HCl (*pH *8). All these procedures were carried out at 4 °C. The neutralized fractions and crude extracts were run in sodium dodecyl sulphate-polyacrylamide gel electrophoresis (SDS-PAGE), subjected to western-blot, and analysed with specific antibodies against GFP or HA epitopes (Roche).*

2.7. Bimolecular Fluorescence Complementation (BiFC) constructs and confocal imaging

To generate the constructs to perform BiFC assays, both cDNAs, *TRXh5* and *TIRK*, were cloned into the Gateway binary destination vectors pXNGW and pXCGW (provided by Dr. Luis Oñate, CBGP-UPM, Spain), harbouring the N- and C-terminal parts of the GFP, respectively. Therefore, each protein was independently tagged with nGFP or cGFP at the C-terminus. The BiFC constructs were introduced into Agrobacterium and then infiltrated in *N. benthamiana* plants as described above. Fluorescent images were acquired 3 d after infiltration using a Leica TCS-SP8 confocal microscope. *GFP and chlorophyll autofluorescence signals were acquired sequentially using the following settings: GFP, excitation* 488 nm *and emission 500*–600 nm*; chlorophyll, excitation* 633 nm*, emission 693*–745 nm.

2.8. Plant damage determination

To study the role of TRXh5 and TIRK in plant defence against spider mites, 3-week-old rosettes from mutant, over-expression, and WT lines were infested with 20 *T. urticae* female adults per plant for 4 d. Damage quantification was performed using an HP scanjet (HP Scanjet 5590 Digital Flatbed Scanner series) as described [39] and leaf damage was calculated in mm^2 using Adobe Photoshop CS software.

2.9. Spider mite performance

To analyse the response of spider mites feeding on WT and *TRXh5* and *TIRK* transgenic plants, fecundity assays were performed. Spider mite female synchronization was conducted as described [13] and then entire detached leaves from the transgenic and WT plants were infested with 12 synchronized females each, and the number of eggs laid was counted after 36 h.

2.10. Quantification of ROS and NO

To determine the accumulation of ROS and nitrogen oxide (NO) *in vivo* upon spider mite infestation, 0.5 mm leaf discs from the *TRXh5*

A

TRXh5

	Bla-2	Kon
1h	1.47	-0.09
3h	1.70	1.21
6h	2.24	1.76
12h	2.06	2.26
24h	1.84	2.09

B

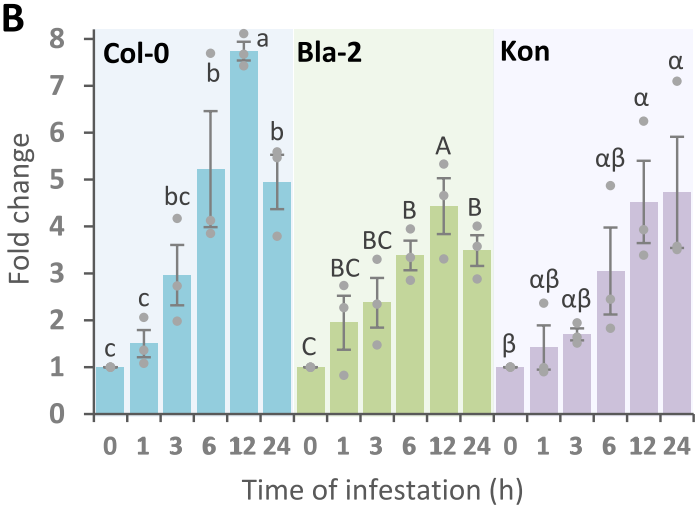

C

TIRK

	Bla-2	Kon
1h	0.65	0.64
3h	0.31	0.43
6h	0.54	0.76
12h	0.54	0.75
24h	0.62	0.79

D

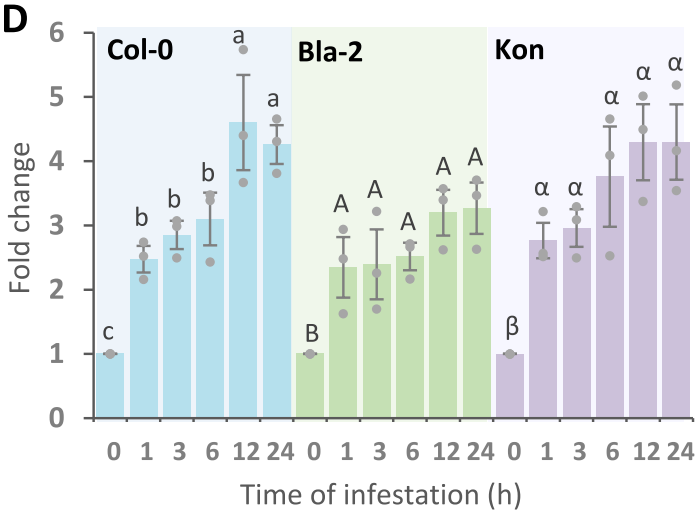

Fig. 1. *TRXh5* and *TIRK* gene expression in response to *T. urticae* infestation. Microarray data of *TRXh5* (**A**) and *TIRK* (**C**) gene expression in Arabidopsis Bla-2 and Kon accessions at 1, 3, 6, 12, and 24 h post-infestation is represented as Log_2 fold change. RT-qPCR assays of *TRXh5* (**B**) and *TIRK* (**D**) gene expression in Arabidopsis Bla-2, Kon and Col-0 accessions at 1, 3, 6, 12 and 24 h post-infestation with *T. urticae*. Gene expression referred to as fold change (2^{-ddCt}) was calculated using the control (0 h) for each genotype as an internal calibrator. Data are means ± SE of three biological replicates. Different letters indicate significant differences between times post-infestation within each accession (One-way ANOVA followed by Newman-Keuls multiple comparisons test, $p < 0.05$).

transgenic lines and WT were infested with 10 adult females per disc for 6 h. Leaf discs were collected and incubated in darkness as described by Ref. [40] with fluorescent probes, 25 μM DCF-DA for 30 min at 37 °C or 10 μM DAF-2 DA for 60 min at 25 °C, to detect ROS and NO, respectively. To control the specificity of the reaction for NO detection, 400 μM Carboxy-PTIO (NO scavenger) before dye staining for 1 h at 25 °C was used. Fluorescence emissions of the probes were sequentially acquired using a Leica TCS-SP8 confocal microscope applying the tile-scan tool to scan the entire leaf disc *using the following settings: DCF-DA, excitation* 488 nm *and emission 493*–562 nm*; DAF-2 DA, excitation* 488 nm *and emission 493*–562 nm*; chlorophyll, excitation* 633 nm*, emission 692*–736 nm. *Fluorescence intensity of the whole leaf disc was quantified using Image J software. In addition,* H_2O_2*-accumulation was analysed by histochemistry using DAB, which produces a brown precipitate after oxidation in the presence of H2O2* [41]. *WT and trxh5 mutant Arabidopsis leaf disks (0.*8 mm *diameter) were infested with 10 mites and incubated for 6 h. Infested and non-infested control discs were stained with* 3,3′-diaminobenzidine (*DAB) according to* Ref. [42]; *observed under a Zeiss Axiophot microscope, and brown precipitates were quantified using the colour deconvolution plug in Image J software. Ascorbic acid (*10 mM*) has been used as ROS scavenger.*

2.11. S-nitrosylation assays

To detect S-nitrosylated proteins, the biotin switch method that converts –SNO into biotinylated groups, was performed according to Ref. [43]. Three-week-old rosettes of *TRXh5* transgenic and WT plants were infested with 20 female adults for 6 h. Arabidopsis rosettes were homogenized in MAE buffer (25 mM HEPES, 1 mM EDTA, 0.1% Triton X-100 (v/v), 0.1 mM neocuproine, pH 7.7) containing a complete protease inhibitor cocktail (Roche) and centrifuged at 4 °C for 30 min. Total protein content was determined using the Bradford method [38]. To block free cysteine, 300 μg of total protein were incubated for 20 min at 50 °C in a blocking solution (25 mM HEPES, 1 mM EDTA, 0.1 mM neocuproine, 2.5% (w/v) SDS, 20 mM methyl-methanethiosulfate, pH 7.7) with frequent vortexing. Excess methyl-methanethiosulfate was removed by cold acetone precipitation and proteins were resuspended in 25 mM HEPES, 1 mM EDTA, and 1% (w/v) SDS, pH 7.7 buffer (100 μl mg^{-1} protein) and then were incubated at room temperature for 1 h in darkness after the addition of 1 mM HPDP-biotin (Thermo Scientific) and 1 mM ascorbic acid. Moreover, GSNO (1 mM) treatment, and samples without biotin or ascorbic acid were used to validate the reliability of the method. Then, western-blot analysis was performed using an anti-biotin antibody (Sigma). To detect S-nitrosylation pattern of

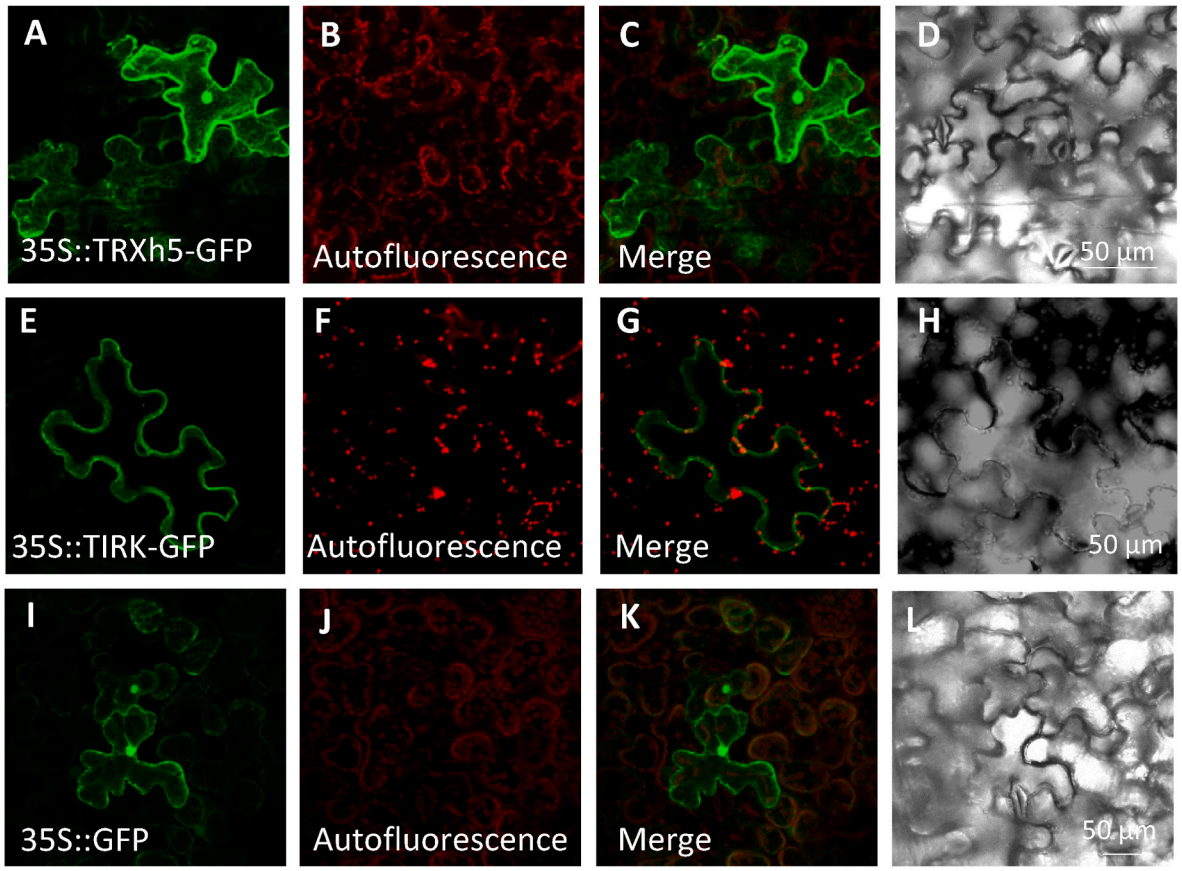

Fig. 2. Subcellular location of TRXh5 and TIRK in *N. benthamiana* leaves. Confocal stacks spanning *N. benthamiana* cells agroinfiltrated with 35S::TRxh5-GFP, 35S::TIRK-GFP and 35S::GFP control. Projections of GFP (**A,E,I**), chlorophyll auto fluorescence (**B,F,J**), merged (**C,G,K**), and the corresponding Nomarski snapshots (**D,H,L**). Scale bars are indicated in the Nomarski images.

TIRK, Arabidopsis extracts from 35S::TIRK-GFP were incubated or not with extracts from the over-expression TRXh5 (2:3), and subjected to the biotin switch method. To purify *in vivo* biotinylated proteins, immunoprecipitation with IPA (protein A/G Ultralink Resin, Pierce)-*anti*-biotin antibody (Sigma) was carried out as described before [44]. Beads were washed with TBS-Tween (0.1%, v/v) buffer and bound proteins were eluted with 10 mM DTT in SDS-PAGE solubilisation buffer, loaded in 8% SDS-PAGE and transferred to a PVDF membrane to detect TIRK-SNO with anti-GFP antibody (Agrisera).

2.12. Hormone determination

Plant hormones 12-oxophytodienoic acid (OPDA), JA, JA-Isoleucine (JA-Ile), and SA were quantified by isotopic dilution mass spectrometry from 3-week-old rosettes of *TRXh5_1.4*, *trxh5_2* and WT plants after 6 h of spider mite feeding. Six rosettes were pooled per experiment and three independent experiments were performed. Isotope-labelled standards were added to lyophilized plant samples (200 mg) prior to extraction as previously described [45]. Ultra-performance liquid chromatography (UPLC)-electrospray ionization tandem mass spectrometry analyses were carried out on an Acquity SDS system (Waters) coupled to a triple quadrupole mass spectrometer (Micromass). Quantification was accomplished with an external calibration.

2.13. Statistics

To design a suitable statistical approach was used GraphPad Prism v6.01 and each poll of data was previously subjected to normality and homoscedasticity tests. When data fulfilled both assumptions, One- or Two-way ANOVA was applied, followed by Student Newman-Keuls multiple comparison test ($p < 0.05$). Two-way ANOVA was performed in the experiments where genotype (G) and treatment with mites (T) were simultaneously analysed and Newman-Keuls multiple comparisons test was used when the interaction (I:G × T) was significant. In the case of S-nitrosylation quantification, data present normal distribution but not homoscedasticity, so an Unpaired *t*-test with Welch's correction ($p < 0.05$) was performed to compare the samples to the WT. Number of replicates are shown in the figure legends.

3. Results

3.1. Gene expression of TRXh5 and TIRK in response to T. urticae infestation

The Arabidopsis accessions Kon and Bla-2 were identified as susceptible and resistant to the mite *T. urticae,* respectively [11]. Among otherwise similar responses, microarray analyses showed consistently different expression levels of the *TRXh5* gene in the Bla-2 strain relative to Kon, at different infestation times (Fig. 1A). RT-qPCR assays confirmed the differential expression of *TRXh5* between accessions and pointed to the remarkable induction of this gene in Col-0 upon spider mite attack (Fig. 1B), involving this thioredoxin in plant response to *T. urticae*.

As the molecular function of TRXh5 involves its interaction with other proteins [46], an *in silico* search for interacting proteins was performed. Direct binding was previously described between TRXh5 and 63 Arabidopsis proteins (BIOGRID database). Thus, these interacting proteins were used to determine enriched GO terms. Using the ClueGO tool, significant enrichments were found for biological processes related to transmembrane transport, kinase activity, and defence (Fig. S1). One of

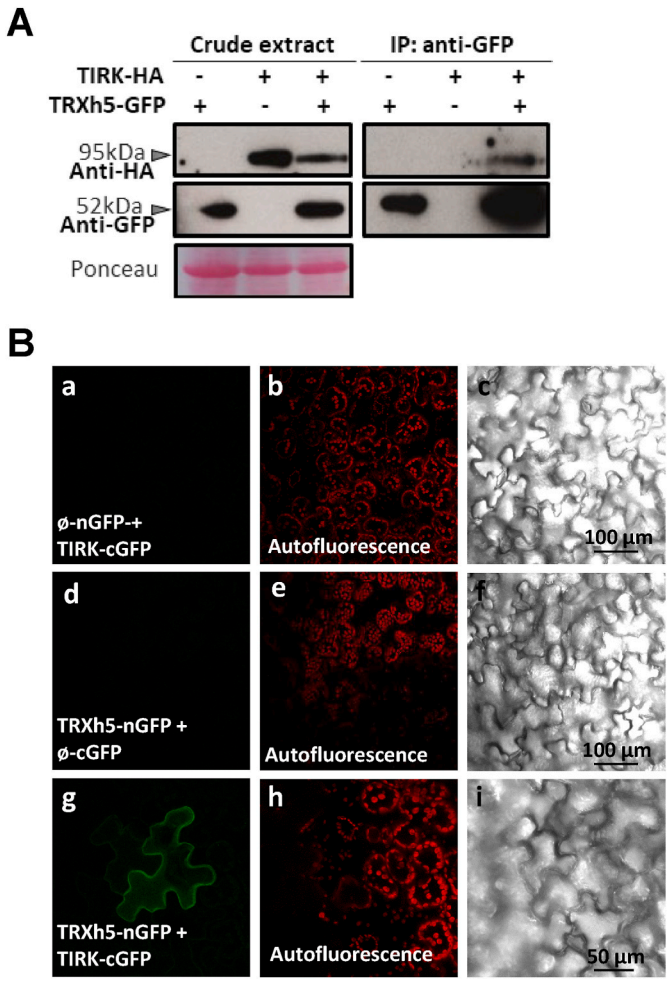

Fig. 3. Protein interaction assays. (**A**) CoIP assay of *N. benthamiana* extracts from leaves transiently expressing *TRXh5-GFP* and *TIRK-HA* under the control of the 35S promoter. The presence of proteins in the crude extracts and in the immunoprecipitated fractions was determined by western-blot analysis using anti-GFP and anti-HA antibodies. The experiments were independently repeated three times with similar results. (**B**) BiFC to analyse TRXh5-TIRK protein-protein interaction. Confocal stacks spanning *N. benthamiana* cells agroinfiltrated with ø-nGFP- + TIRK-cGFP (a) N- TRXh5-nGFP + ø-cGFP (d) and TRXh5-nGFP + TIRK-cGFP (g). Projections of GFP (a,d,g), chlorophyll autofluorescence (b,e,h), and the corresponding Nomarski snapshots (c,f,i). Bars are indicated in the Nomarski images.

these proteins, encoded by the *At5G10290* gene, was a RLK receptor with an extracellular LRR domain and an intracellular kinase domain, previously shown to be induced by *T. urticae* feeding [11], although it was not functionally characterized. Thus, we were interested in this protein as no receptors involved in HAMPs detection has been described in the plant-mite context. This protein named THIOREDOXIN INTERACTING RECEPTOR KINASE and referred from now on as TIRK, is regulated by a bidirectional promoter that specifically responds to biotic stresses [47]. RT-qPCR assays supported the induction of *TIRK* in the Bla-2 and Kon accessions at different mite infestation times and established a similar pattern of expression in the Col-0 accession (Fig. 1C and D), suggestion a possible role for TIRK in plant response to *T. urticae*.

3.2. Tissue expression of TRXh5 and TIRK genes and subcellular protein localization

To analyse the distribution of TRXh5 and TIRK in the plant, the expression of *TRXh5* and *TIRK* genes in different tissues was assessed. RT-qPCR assays demonstrated the expression of both genes in all analysed tissues, including rosette leaves, the main source of nutrients for mite feeding (Fig. S2). Consistent with their putative roles in signalling vs ligand perception, the levels of *TRXh5* transcripts were much higher than *TIRK* levels.

Transient expression assays were conducted to determine whether TRXh5 and TIRK proteins colocalize in the same subcellular compartment. Agroinfiltration of the open reading frame of *TRXh5* translationally fused to the GFP in *N. benthamiana* leaves showed the accumulation of TRXh5-GFP throughout the entire endoplasmic reticulum (ER) network, which was continuous with the nuclear envelope. The TRXh5-GFP protein was also detected in the plasma membrane, cytoplasm, and within the nucleus (Fig. 2A–D). Consistent with the putative role as a receptor kinase, *N. benthamiana* agroinfiltration experiments showed the TIRK-GFP localization exclusively in the plasma membrane (Fig. 2E–H). A possible cytosolic location of TIRK protein was observed in the confocal stacks spanning (Fig. 2E) but it was due to the z-projections of multiple z-planes and the 3D structure of the cell. In the individual focal planes, the location of TIRK is only detected in the membranous system of the cell (Fig. S3 and Fig. S4). As expected, the GFP control showed fluorescence throughout the cell (Fig. 2I-L). The autofluorescence of the chloroplast did not merge with the fluorescence emitted by GFP detected in the endomembrane system or in the plasma membrane. *T*ransient expression assays in *A. cepa* corroborated localization patterns of TRXh5-GFP and TIRK-GFP proteins (Fig. S5). Plasmolysis induced by 1 M mannitol treatment confirmed the location of TRXh5 and TIRK in the cell wall-detached plasma membrane, with no fluorescence observed either in the cell wall or in the apoplast (Figs. S5E–H,M – P). These results together showed that both proteins colocalize in the plasma membrane and allow us to think about a possible interaction between them, supporting the *in silico* results.

3.3. The TRXh5 protein interacts with the RLK receptor TIRK

To confirm *in vivo* the interaction reported between TRXh5 and TIRK, we performed to independent techniques such as Co-immunoprecipitation (CoIP) and BiFC assays. For CoIP assays, crude extracts of co-agroinfiltrated *N. benthamiana* leaves transiently expressing the TRXh5 protein fused to GFP (TRXh5-GFP) and the TIRK protein fused to HA (TIRK-HA) were immuno-precipitated with the anti-GFP antibody, and the precipitate contained both proteins, as detected by anti-GFP and anti-HA antibodies (Fig. 3A), demonstrating their interaction. Controls expressing only one of these proteins and pulled down with the anti-GFP antibody precipitated only TRXh5-GFP, but not TIRK-HA (Fig. 3A). In BiFC experiments, GFP fluorescence was observed only when both proteins were simultaneously co-agroinfiltrated in *N. benthamiana* plants (Fig. 3B). As expected, from TIRK localization, this fluorescence was detected in the plasma membrane. No overlap was found with chlorophyll autofluorescence, and Nomarski images supported the integrity of the cells (Fig. 3B). All these results together corroborated the physical interaction between TRXh5 and TIRK *in planta*.

3.4. TRXh5 and TIRK proteins are required for Arabidopsis defence against T. urticae

Induction of *TRXh5* and *TIRK* gene expression by mite infestation and their protein-protein interaction suggested a coordinated defensive role in Arabidopsis against spider mites. To test this role, we characterized two homozygous Arabidopsis insertion lines, *trxh5_1* (T-DNA insertion in the 5′UTR leading to a reduced expression of *TRXh5* gene) and *trxh5_2* (T-DNA insertion in the second exon, resulting in gene knock-out, Figs. S6A and D). Several Arabidopsis lines over-expressing the *TRXh5* gene were also generated and *TRXh5* expression was analysed by qRT-PCR assays as shown in Fig. S6E. Among all the lines analysed, *TRXh5_1.4* and *TRXh5_3.3* were selected based on their expression prole for further studies. Homozygous T-DNA insertion lines

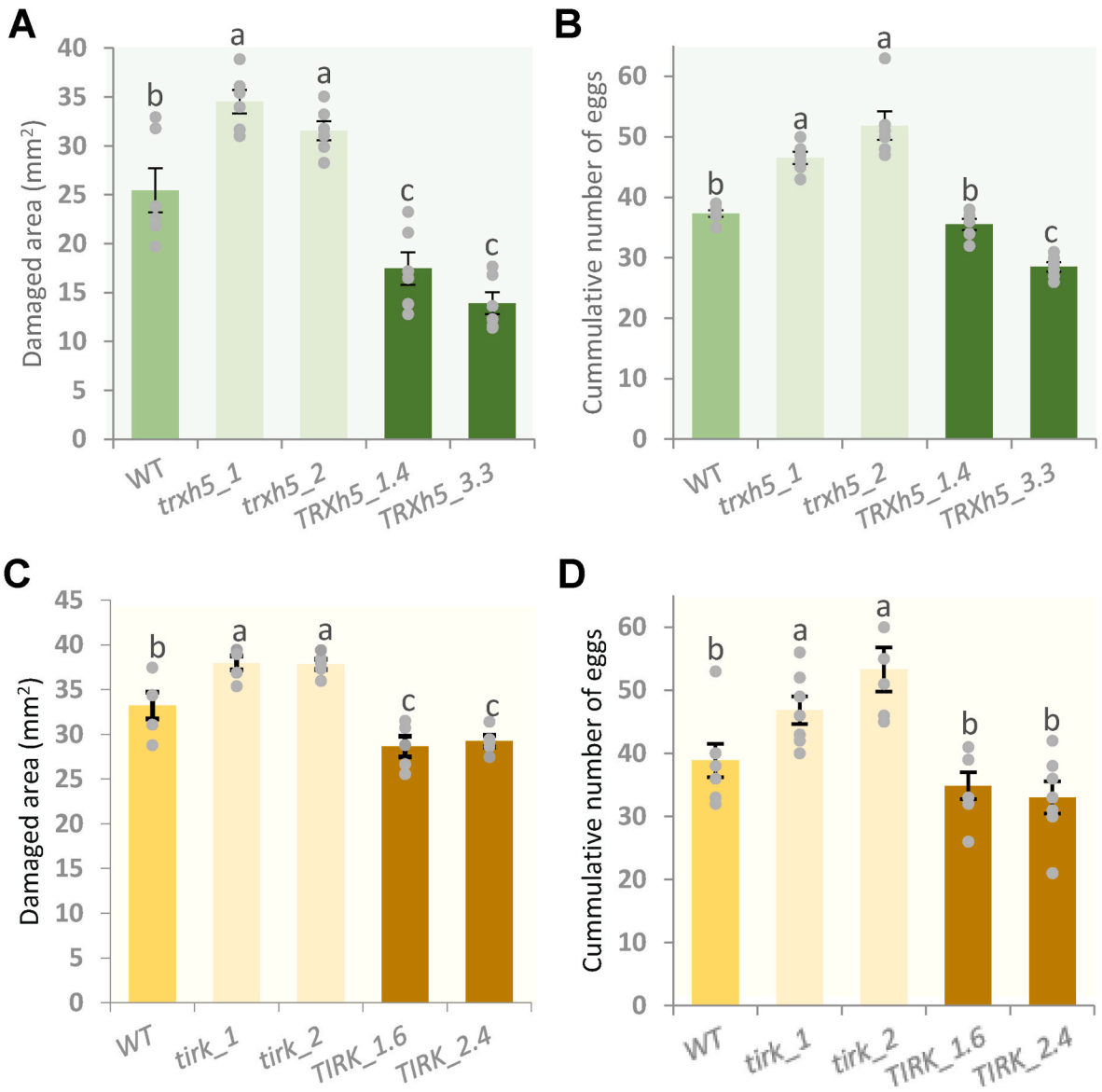

Fig. 4. Plant damage after mite infestation and mite fecundity upon feeding on WT, *TRXh5* and *TIRK* over-expression and mutant lines. (A) Foliar area damaged in WT, *TRXh5* over-expression and *trxh5* mutant lines 4 d after mite infestation. (**B**) Mite fecundity 36 h after feeding on WT, *TRXh5* over-expression and *trxh5* mutant lines. (**C**) Foliar area damaged in WT, *TIRK* over-expression and *tirk* mutant lines 4 d after mite infestation. (**D**) Mite fecundity 36 h after feeding on WT, *TIRK* over-expression and *tirk* mutant lines. Data are means ± SE of six replicates. Different letters indicate significant differences (One-way ANOVA followed by Student-Newman-Keuls test, $p < 0.05$).

and over-expression lines, as well as the corresponding WT plants, were infested with mites and plant damage was quantified after 4 d of mite feeding. The two *TRXh5* over-expression lines showed the least damage, followed by the non-transformed WT plants, while the damaged area was greatest in the knockdown *trxh5* lines (Fig. 4A). Mite fecundity followed a similar pattern. It was the highest when mites fed on *trxh5* plants and the lowest when they fed on *TRXh5*-over-expression lines (Fig. 4B). Thus, *TRXh5* functions to protect Arabidopsis against mite attack.

To further determine the role of the TIRK protein in plant defence, feeding bioassays with *TIRK* loss- and gain-of-function lines were also performed. The knock-out line *tirk*_1 had the T-DNA insertion into the second intron and the knock-down line *tirk_2* in the 5′UTR (Fig. S7). Similar to TRXh5 over-expression lines, several Arabidopsis lines over-expressing *TIRK* gene were genrated and TIRK expression was analysed by qRT-PCR as shown in Fig. S7E. Homozygous *tirk_1* and *tirk_2* insertion lines, selected *TIRK_1.6* and *TIRK_2.4* over-expression lines, and WT plants were infested with mites and plant damage was measured after 4 d of feeding. *TIRK*-over-expression plants were significantly less damaged than WT plants and *tirk* mutant lines incurred more injury than controls (Fig. 4C). Concomitantly, the cumulative number of eggs was significantly greater in *tirk* mutant lines than in WT (Fig. 4D), demonstrating the defensive function of the TIRK receptor.

3.5. Transcriptional expression of TRXh5 and TIRK genes within transgenic lines of the other partner

Because *TRXh5* and *TIRK* genes were up-regulated in WT plants by mite infestation, their encoding proteins interacted, and both conferred resistance to *T. urticae*, the altered expression of each gene could affect the expression of its partner. Thus, the expression pattern of both genes was studied by RT-qPCR in the different Arabidopsis genotypes. A significant increase in *TRXh5* transcripts was observed in non-infested *TIRK* over-expression and *tirk* mutant lines in comparison to WT plants

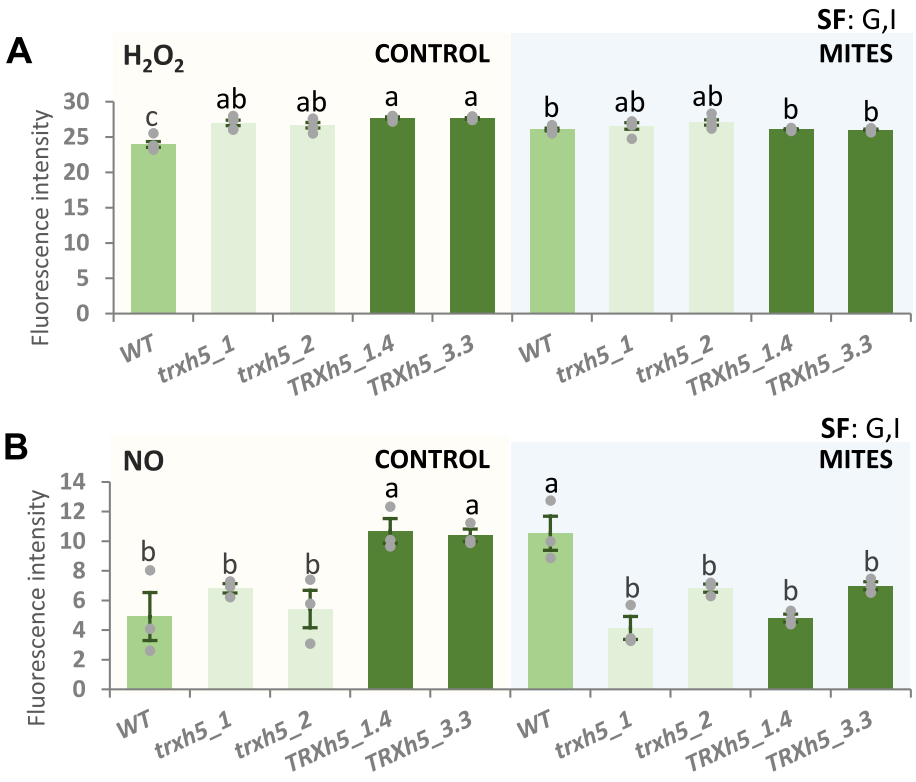

Fig. 5. The effects of mite interaction on ROS and NO levels in WT, TRXh5 over-expression and trxh5 mutant lines. (**A**) ROS-dependent DCF-DA and (**B**) NO-dependent DAF-2-DA fluorescence intensity upon 6 h after mite infestation. Data are means ± SE of three biological replicates. Significant factors (SF) indicate whether the two independent factors, T (mite treatment) and G (genotype), and/or their interaction, I (TxG), were statistically significant (Two-way ANOVA, $p > 0.05$). When the interaction was not significant, Student-Newman-Keuls test was performed.

(Fig. S8A, inserted panel), while *TIRK* gene expression was not altered in *TRXh5* over-expression and *trxh5* mutant lines (Fig. S8B). After mite infestation, the expression of both *TRXh5* and *TIRK* increased independently of the Arabidopsis transgene background (Figs. S8A and B). These results indicate that alterations in the expression of the *TIRK* gene modulate the expression of *TRXh5*.

3.6. Transcriptional expression of the cytosolic thioredoxins in trxh5 mutant backgrounds

Since the Arabidopsis genome contains eight cytosolic thioredoxins (genes *TRXh1* to *h9)*, alterations in the expression of *TRXh5*, both at basal levels and upon spider mite infestation, might cause compensatory effects within this gene family. Thus, the expression of the cytosolic *TRXh1* to *h9* genes was checked in *trxh5_1* and *trxh5_2* mutants and in WT plants. No significant differences were found in the transcript levels of these genes except for the *TRXh1* gene, which had slightly higher expression levels after 6 h of mite treatment in WT than in *trxh5* mutant lines (Fig. S9). These results support that the *trxh5_1* and *trxh5_2* mutant genotypes were mainly associated with the perturbed function of the *TRXh5* locus, and suggest that TRXh5 may have a specific role not overlapping with other thioredoxins h-type.

3.7. Changes in TRXh5 expression are associated with variations in the accumulation of ROS and NO, and with the S-nitrosylation pattern

As thioredoxins are involved in redox homeostasis, the defensive role of the TRXh5 is expected to be linked to changes in ROS and/or RNS accumulation. Thus, the levels of ROS and NO molecules were measured in different *TRXh5* genotypes after 6 h of spider mite infestation. This infestation time was selected because it corresponds to the check-point marking differences in gene expression in Bla-2 vs Kon (Fig. 1). Using fluorescence-based assays and the confocal microscopy, we quantified the ROS and NO levels in the different genotypes. Additionally, H_2O_2 was localized by using DAB (Fig. S10), and precipitates quantification lead to similar results to ROS. The accumulation of ROS and NO were influenced by both Arabidopsis genotypes and mite infestation (Fig. 5 and Fig. S10). Despite complexity, we observed the following patterns: i) levels of both ROS and NO increased in the WT upon mite infestation; ii) even though levels of ROS increased and levels of NO decreased in T-DNA insertion lines relative to non-transformed control, they were not affected by mite infestation state; iii) levels of both ROS and NO increased in *TRXh5* over-expression lines in the absence of mites, but decreased upon mite infestation.

As TRXh5 has been shown to have selective protein denitrosylation activity involved in plant immunity [48], we further checked if differences in the redox levels between Arabidopsis genotypes might be linked to protein S-nitrosylation mediated by the thioredoxin. Thus, we analysed the S-nitrosylation pattern of the different lines using the biotin switch method, converting unstable S–NO groups into more stable biotinylated groups. The immunoblots, using an anti-biotin antibody, revealed different levels of biotinylated proteins among *TRXh5* genotypes (Fig. 6). In WT plants, quantification of the signal associated with S-nitrosylated proteins showed an increase after 6 h of treatment to decrease at 24 h of treatment. Notably, depending on the Arabidopsis genotype the signal detected in our assay differed. While an increase of the signal related to S-nitrosylated proteins was observed in *trxh5* mutant lines respect to WT, in *TRXh5* over-expression lines S-nitrosylated proteins practically disappeared (Fig. 6). The addition of GSNO and the absence of biotin or ascorbate in the experimental reaction confirmed the attribution of the detected bands to S-nitrosylated proteins (Fig. S11). These results support the participation of TRXh5 in redox homeostasis that affects a wide range of proteins in a TRXh5-concentration dependent manner.

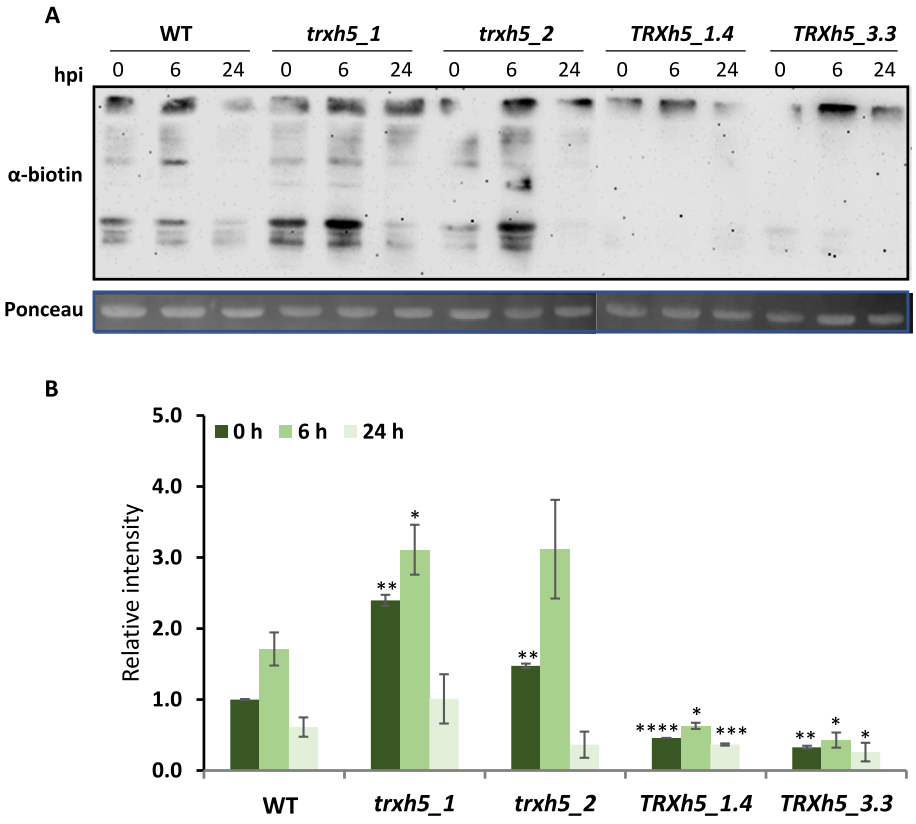

Fig. 6. S-nitrosylated proteins upon mite infestation in WT, *TRXh5* over-expression and *trxh5* mutant lies. (**A**) In-gel detection of S-nitrosylated proteins in extracts of Arabidopsis WT and *TRXh5* transgenic lines at 0, 6 and 24 h post-infestation (hpi) and subjected to the biotin switch method. (**B**) Band intensity quantification relative to Ponceau intensity. Asterisk number indicates significant differences compared to the WT (0 h). Unpaired *t*-test with Welch's correction ($p < 0.05$).

3.8. S-nitrosylation pattern of TIRK

As TRXh5 is able to reverse SNO modifications [48], and in our *TRXh5* over-expression lines, S-nitrosylation signal practically disappears, we further explored whether TIRK is S-nitrosylated *in vivo* and if TRXh5 is able to regulate S-nitrosylation pattern of this receptor. Therefore, protein extracts from 35S::TIRK-GFP plants, incubated for 30 min or not with extracts from the *TRXh5* over-expressipn line were assayed by the biotin switch method. Western-blot analysis on S-nitrosylated purified protein with an anti-GFP antibody showed the corresponding S-nitrosylation state of TIRK *in vivo*. S-nitrosylation signal of TIRK decrease in the presence of TRXh5 over-expression line extracts (Fig. 7), suggesting that TRXh5 is a redox regulator of the receptor. UV-induced SNO photolysis was used as a control (Fig. 7).

3.9. Hormonal responses in Arabidopsis TRXh5 altered backgrounds

Since ROS, RNS and redox-dependent posttranslational modifications (PTMs) regulate the activation of several hormonal signalling pathways, the accumulation of hormones related to defensive pathways, such as OPDA, JA, JA-Ile and SA, were measured in leaves infested and non-infested with mites (Fig. 8). The levels of OPDA showed non-significant variations between infested and non-infested plants independently of the plant genotype. JA accumulated in leaf tissues after 6 h of mite infestation in the three Arabidopsis genotypes. However, this accumulation was significantly higher in plants over-expression the *TRXh5* gene, suggesting that TRXh5 modulated the JA biosynthesis/signalling pathway. In contrast, JA-Ile content increased in infested WT plants relative to the non-infested plants, but it did not show differences in *TRXh5_3.3* and *trxh5_2* lines either in the presence or absence of mites. Regarding SA content, only a reduction tendency was observed in the *TRXh5* mutant line after 6 h of infestation.

4. Discussion

The diversity of mechanisms used by TRXs to regulate plant immunity represents a challenging issue that is currently the focus of defence signalling research studies [5,6]. These proteins not only reduce S-nitrosothiols (-SNO), S-sulfenic acids (-SOH), and disulfides (S–S) to allow ROS and RNS signalling but also bind cysteine residues to guard critical proteins. To date, TRXh5 has been associated with the Arabidopsis response to different abiotic and biotic stresses. Among biotic stimuli, *TRXh5* gene expression was up-regulated during incompatible interactions with the bacterial pathogen *Pseudomonas syringae* [49]. A transcriptomic data analysis reported induction of *TRXh5* expression in response to the necrotrophic fungus *Botrytis cinerea*, the oomycetes *Phytophthora infestans* and *Hyaloperonospora parasitica* [50]. Recently, we have reported that the induced expression of *TRXh5* was associated with herbivory by a range of arthropods belonging to different guilds, such as the acarian *T. urticae*, the lepidopteran *Pieris rapae*, and the thrip *Frankliniella occidentalis* [51]. Here, using *trxh5* mutants and *TRXh5* over-expression plants, we confirm the role of TRXh5 in Arabidopsis defence against *T. urticae*. While over-expression plants were less damaged and accumulated a lower number of *T. urticae* eggs than WT plants, *trxh5* mutants were more injured and a higher number of eggs was detected in these plants.

Our findings show that plants with altered expression of TRXh5 show disturbance in ROS homeostasis with slightly accumulation in both, silenced mutants and *TRXh5* over-expression plants under control conditions. As thioredoxins are involved in H_2O_2 scavenging [2,52,53],

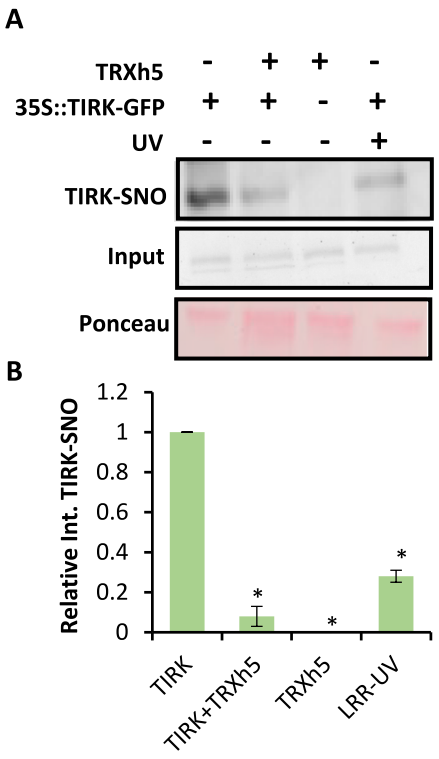

Fig. 7. S-nitrosylation pattern of TIRK. (**A**) *In vivo* analysis of S-nitrosylation pattern of TIRK in 35S::TIRK-GFP lines incubated or not with extracts from over-expression line TRXh5. Protein extracted from 2-weeks-old 35S::TIRK-GFP seedlings incubated or not with extracts from TRXh5 over-expression line, and extracts from only the TRXh5 seedlings were subjected to biotin-switch assay, immunoprecipitated with anti-biotin antibody and TIRK was identified by an anti-GFP antibody after western-blotting of the biotinylated proteins (TIRK-SNO). The sample from TIRK-GFP seedlings pre-treated with UV served as negative control. (**B**) Quantification of two independent western-blots. Asterisks denote significant differences between samples and TIRK-GFP plants according to Student's *t*-test ($p < 0.05$).

higher amounts of TRXh5 protein are expected to be associated with low H_2O_2 although compensatory effects for constitutive over-expression may have induced H_2O_2 production. As previously reported [12], H_2O_2 levels increased upon mite treatment. However, while we have shown that *trxh5* mutants maintained an elevated level of ROS, *TRXh5* over-expression plants decreased the amount of ROS upon mite infesttaion. In the case of NO, no increase in this molecule was observed upon mite treatment in *trxh5* mutants, probably due to the absence of normal denitrosylation activity. Surprisingly, the interaction of mites and *TRXh5* over-expression plants led to a decrease in NO content despite the positive effect on NO accumulation provoked by both mite stress and TRXh5 activity. Above a certain threshold, NO and ROS would trigger plant cell death, while below this threshold would act as signalling molecules [54,55]. Therefore, the elevated basal levels of NO and ROS detected in *TRXh5*-over-expression plants are expected to trigger rapid activation of signalling pathways that must be promptly stopped to avoid toxicity. This rapid activation may correlate with a minor susceptibility to the spider mite and a higher increase in JA levels.

An increase in ROS generation was found in the yeast *Candida albicans* treated with the TRXh5 protein, which was associated with the inhibition of fungal growth production [56]. Likewise, NO and H_2O_2 levels regulate the accumulation of defence-related hormones such as JA and SA. Increased levels of ROS or RNS lead to the activation of the JA and SA pathways [55,57]. Therefore, higher levels of H_2O_2 and NO levels are expected to affect the basal levels of JA and SA hormones. However, these levels were similar in plants with different basal expression of *TRXh5*, suggesting that additional regulatory pathways modulate the effect of NO and H_2O_2 on hormonal induction. Interestingly, JA content increased in response to mites in all genotypes, mainly in *TRXh5* over-expression lines. Taking into account the absence of changes in OPDA, a precursor of JA synthesized in chloroplasts, the increase of JA could be due to activation of peroxisomal β-oxidation. This hypothesis is supported by the up-regulation of *Acyl-CoA oxidase 1* (*ACX1*) observed in the transcriptome carried out in plant response to *T. urticae* [58]. ACX1 is a key enzyme involved in JA biosynthesis and can be regulated by phosphorylation and ROS- and NO-dependent PTMs [59], although the mechanisms have not been described so far.

In addition, TRXh5 was reported to physically interact *in silico* with the cytosolic NPR1 oligomers. Upon activation of SA signalling, TRXh5 facilitates the denitrosylation of NPR1 oligomers, realising NPR1 monomers for translocation into the nucleus where they activate SA-responsive immune gene [20,48]. Our results showed a significant role for TRXh5 denitrosylation activity as supported by the decrease in the S-nitrosylation dependent signal observed in the *TRXh5* over-expression plants, and according to previous results that showed TRXh5 contribution to protein denitrosylation activity in plant cells [48]. Lower levels of S-nitrosylation in *TRXh5* mutants may explain higher NO levels observed in the mutants under control conditions. However, differential regulation of NO metabolism may occur in these lines, under control and stress conditions, affecting to nitrate reductase, and/or nitrosoglutathione reductase, being both of them regulated by S-nitrosylation. As it has been shown previously, NO regulates its own homeostasis in a complex way that remains to be completely elucidated [60,61]. More evidences suggest however, that NPR1 acts as a central hub for immune response, acting also downstream JA and ethylene during development of induced resistance [62], and regulating defence hormone crosstalk [63,64]. These results suggest that TRXh5 has a central role in the regulation of plant immune responses, which may be involved in different hormone-dependent signalling pathways.

The subcellular location of TRXh5 in the cytosol, the membrane systems and the nucleus is compatible within a scenario in which TRXh5 interacts with diverse proteins to control various physiological processes. Consistently, TRXh5 was reported to physically interact *in silico* with at least 63 proteins, being one of them the LRR-receptor TIRK. Interactions between TRXh5 and membrane-associated proteins have been described, mainly transmembrane transporters and kinase-like receptors. This is the case of the NB-LRR (LOV1) receptor [22]. The role of LOV1 in plant immunity is supported by LOV1-mediated cell death triggered by the necrotrophic fungus *C. victoriae*, which secretes a toxin that binds to TRXh5 at the active site Cys39, causing the release of LOV1 [22]. This example supports the role of TRXh5 as a guardee of client proteins involved in the perception of foreign stimuli and as a regulator of signalling pathways. Interestingly, genes coding for some of these kinase-like receptors were induced upon mite infestation [58]. While *CRK14*, *CRK31*, and *LECRK62* showed a notable induction upon 30 min of mite infestation, *CRK2*, *WAK3*, and *TIRK* showed a moderate but significant up-regulation in response to the mite treatment. As TIRK encodes a protein previously uncharacterized, it was selected as an excellent candidate for further analysis of the physiological function of the TRXh5-RLK interactions. In fact, TRXh5 and TIRK do not only share their induction by mite infestation and colocalize in the plasma membrane, but we demonstrate that they interact as shown by *in vivo* BiFC and CoIP assays. In addition, alterations in *TIRK* levels, either by over-expression or silencing this gene, modify the basal expression pattern of the *TRXh5* gene.

TIRK belongs to the LRRII-RLK subfamily, formed by three subgroups, the SERK receptors, the NIK1-like receptors, and three receptors with unknown functions [65]. Among the SERKs, SERK3/BAK1, together with SERK4, functions as a co-receptor of several RLKs related to plant immunity, such as the bacterial sensors FLS2 and EFR or the receptors of the plant-derived elicitors PEPR1 and PEPR2 [66]. In contrast, NIK1 positively regulates antiviral activity and has a negative

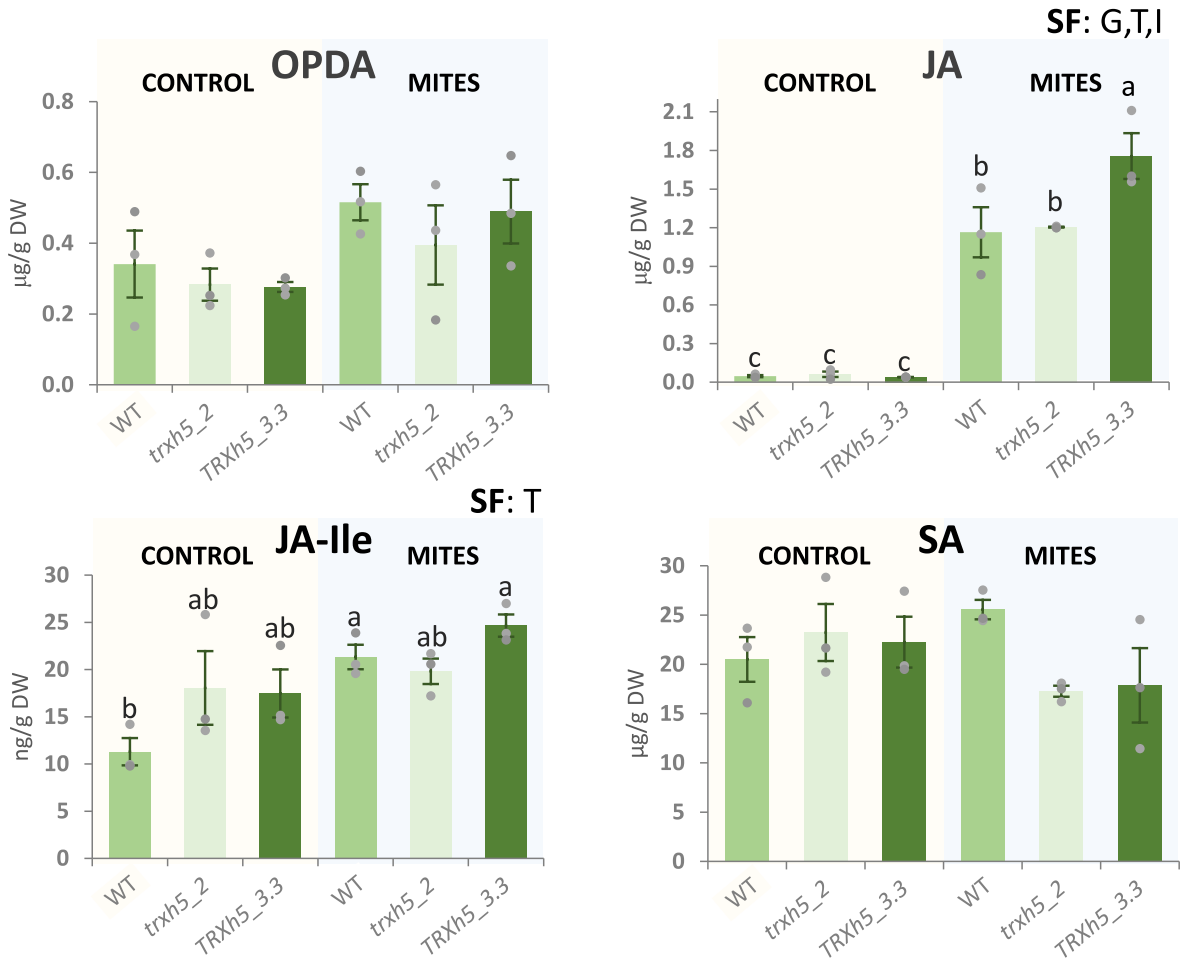

Fig. 8. Quantification of hormone levels after 6 h of *T. urticae* infestation in WT, *TRXh5* over-expression and *trxh5* mutant lines. OPDA, JA, JA-Ile, and SA accumulations are expressed as µg or ng of hormone per g of dry weight (DW). Data are means ± SE of three biological replicates. Significant factors (SF) indicate whether the two independent factors, T (treatment with mites) and G (genotype), and/or their interaction, I (T × G), were statistically significant (Two-way ANOVA, $p > 0.05$). When the interaction was not significant, Student-Newman-Keuls test was performed.

role in antibacterial immunity by interacting with the BAK1/FLS2 complex [67]. TIRK belongs to the third group of RLKs with an unknown function. The members of this group share a short extracellular LRR domain with the SERK and NIK-like receptors, suggesting a role in the perception machinery. Consistent with this regulatory role, the interaction of TIRK with at least 38 RLKs has been reported [68]. Furthermore, two of these interactors, RLK7 and SIF4, have been related to immune responses and their coding genes are rapidly induced upon mite treatment [58,69,70]. Whether these interactions lead to activation of ligand-receptor complexes triggering phosphorylation cascades remains to be elucidated. In any case, increased damage of *tirk* mutant leaves caused by mite feeding and higher mite fecundity in these plants demonstrate the role of TIRK in the establishment of the Arabidopsis defence response to mite attack. In summary, the *TRXh5* and *TIRK* genes are induced by mite infestation and encode interacting proteins necessary for the establishment of Arabidopsis resistance to *T. urticae*. Furthermore, TRXh5 interacts with TIRK and is able to regulate the redox state of the receptor. Thus, we showed that TIRK is S-nitrosylate *in vivo* and that in the presence of TRXh5 over-expression lines, the S-nitrosylation pattern of TIRK decreases. Computational prediction by GPSNO [71] point to Cys409 in the cytoplasmic kinase domain of TIRK as a possible target of S-nitrosylation. In many cases, the interaction between S-nitrosylation and phosphorylation has been described in animal tissues, and in particular, the regulation of kinase activity by S-nitrosylation leading to the suppression of protein kinase activity, the disruption of the interaction with the substrate, the change of

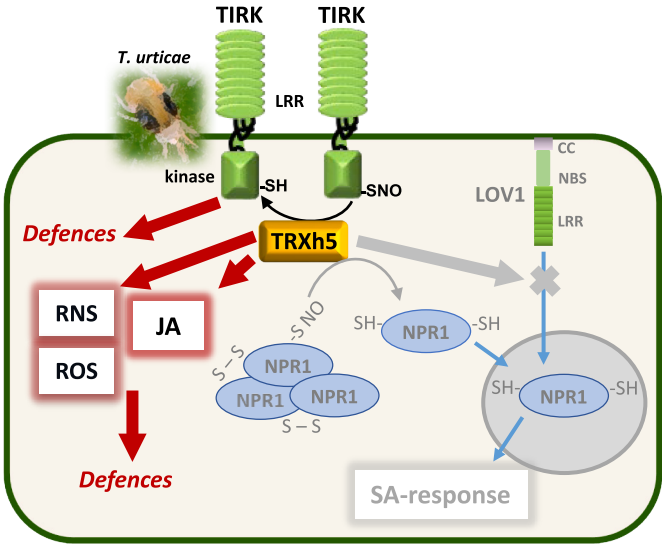

Fig. 9. Schematic representation of the current knowledge on the participation of TRXh5 in plant defence. Pathways associated with the response to the mite are in red colour. (For interpretation of the references to colour in this figure legend, the reader is referred to the Web version of this article.)

localization or even the conversion from kinase into S-nitrosylase [72]. Whether S-nitrosylation may affect TIRK activity, localization or substrate specificity need further analyses however.

5. Conclusions

In conclusion, our results point to a TRXh5-dependent complex network of interactions as possible targets that regulate diverse activities. Presumably, TRXh5 modulates the establishment of Arabidopsis defences against mite herbivory at different steps of signal transduction, from the perception of mite feeding, represented by its interaction with the TIRK protein, to the regulation of gene transcription through redox PTMs of key proteins involved in immune response (Fig. 9). The future challenge is to understand if and how TRXh5 discriminates between its putative protein targets and modulates plant responses to optimize Arabidopsis defence against the two-spotted spider mite *T. urticae*.

Authors' contributions

ID, MCRP and MM conceived the research and wrote the manuscript. AA, MCRP, MES, IRD, VA, AM, VG, PGM, MMC, LMS and MM performed the experimental research and/or contributed to the analysis and interpretation of data. All authors participated in the final version of the manuscript.

Funding

Grants PID2020-115219RB-I00, RED2018-102397-T and RyC17-MESFB funded by MCIN/AEI/10.13039/501100011033, as appropriate, by "ERDF A way of making Europe" and by the "European Union" supported this work. Grants, S0IMQG-263-1HWZ8Q UPM-Banco Santander Universidades, RyC2017-21814 and PRE2018-083375 from MCIN/AEI supported AA, MES and IRD, respectively. The Spanish Ministry of Science and Innovation (MCIN), the State Research Agency (AEI) and the European Regional Development Fund (ERDF; grant MEC-PID2021-122280NB-I00) financed MCRP and LMS. The Government of Canada through the Ontario Research Fund (RE08-067) and the Natural Sciences and Engineering Research Council of Canada (NSERC, RGPIB-2018-04538) supported VG.

Declaration of competing interest

Since plant redox homeostasis and signalling are essential events for the establishment of defence responses to herbivores, we have investigated the role of a cytoplasmic thioredoxin (TRXh5) in the plant-*Tetranychus urticae* interplay.

- TRXh5 participates at different steps of signal transduction, from the perception of mite feeding, represented by its interaction with the TIRK-receptor protein (THIOREDOXIN INTERACTING RECEPTOR KINASE).
- TRXh5 regulates of gene transcription through redox post-translational modifications, particularly S-nitrosylation of proteins involved in the immune response.

Altogether, these findings add new players in the Arabidopsis defense process against phytophagous pests and allow a wider understanding of what is behind the interaction.

Data availability

Data will be made available on request.

Appendix A. Supplementary data

Supplementary data to this article can be found online at https://doi.org/10.1016/j.redox.2023.102902.

References

[1] A. Holmgren, Thioredoxin, Annu. Rev. Biochem. 54 (1985) 237–271.
[2] T. Jedelská, L. Luhová, M. Petřivalský, Thioredoxins: emerging players in the regulation of protein S-nitrosation in plants, Plants 9 (2020) 1426.
[3] Y. Meyer, C. Belin, V. Delorme-Hinoux, J.P. Reichheld, C. Riondet, Thioredoxin and glutaredoxin systems in plants: molecular mechanisms, crosstalks, and functional significance, Antioxidants Redox Signal. 17 (2012) 1124–1160.
[4] P. Geigenberger, I. Thormählen, D.M. Daloso, A.R. Fernie, The unprecedented versatility of the plant thioredoxin system, Trends Plant Sci. 22 (2017) 249–262.
[5] C. Mata-Pérez, S.H. Spoel, Thioredoxin-mediated redox signalling in plant immunity, Plant Sci. 279 (2019) 27–33.
[6] J.R. Bleau, S.H. Spoel, Selective redox signaling shapes plant-pathogen interactions, Plant Physiol. 186 (2021) 53–65.
[7] P.I. Kerchev, B. Fenton, C.H. Foyer, R.D. Hancock, Plant responses to insect herbivory: interactions between photosynthesis, reactive oxygen species and hormonal signalling pathways, Plant Cell Environ. 35 (2012) 441–453.
[8] A. Arnaiz, I. Rosa-Diaz, M.C. Romero-Puertas, L.M. Sandalio, I. Diaz, Nitric oxide, an essential intermediate in the plant-herbivore interaction, Front. Plant Sci. 11 (2021), 620086.
[9] M.E. Santamaria, A. Arnaiz, B. Velasco-Arroyo, V. Grbic, I. Diaz, M. Martinez, Arabidopsis response to the spider mite *Tetranychus urticae* depends on the regulation of reactive oxygen species homeostasis, Sci. Rep. 8 (2018) 9432.
[10] E. Stahl, O. Hilfiker, P. Reymond, Plant-arthropod interactions: who is the winner? Plant J. 93 (2018) 703–728.
[11] V. Zhurov, M. Navarro, K.A. Bruinsma, V. Arbona, M.E. Santamaria, M. Cazaux, N. Wybouw, E.J. Osborne, C. Ens, C. Rioja, et al., Reciprocal responses in the interaction between Arabidopsis and the cell-content-feeding chelicerate herbivore spider mite, Plant Physiol. 164 (2014) 384–399.
[12] M.E. Santamaria, M. Martinez, A. Arnaiz, F. Ortego, V. Grbic, I. Diaz, MATI, a novel protein involved in the regulation of herbivore-associated signaling pathways, Front. Plant Sci. 8 (2017) 975.
[13] M.E. Santamaria, M. Martinez, A. Arnaiz, C. Rioja, M. Burow, V. Grbic, I. Diaz, An Arabidopsis TIR-lectin two-domain protein confers defense properties against *Tetranychus urticae*, Plant Physiol. 179 (2019) 1298–1314.
[14] A. Arnaiz, L. Talavera-Mateo, P. Gonzalez-Melendi, M. Martinez, I. Diaz, M. E. Santamaria, Arabidopsis kunitz trypsin inhibitors in defense against spider mites, Front. Plant Sci. 9 (2018) 986.
[15] A. Schweighofer, V. Kazanaviciute, E. Scheikl, M. Teige, R. Doczi, H. Hirt, M. Schwanninger, M. Kant, R. Schuurink, F. Mauch, et al., The PP2C-type phosphatase AP2C1, which negatively regulates MPK4 and MPK6, modulates innate immunity, jasmonic acid, and ethylene levels in Arabidopsis, Plant Cell 19 (2007) 2213–2224.
[16] G. Romero-Hernandez, M. Martinez, Opposite roles of MAPKKK17 and MAPKKK21 against *Tetranychus urticae* in Arabidopsis, Front. Plant Sci. 13 (2022), 1038866.
[17] E. Widemann, K. Bruisma, B. Walshe-Roussel, R.K. Saha, D. Letwin, V. Zhurov, M. A. Bernards, M. Grbic, V. Grbic, Multiple indole glucosinolates and myrosinases defend Arabidopsis against *Tetranychus urticae* herbivory, Plant Physiol. 187 (2021) 116–132.
[18] A. Arnaiz, M.E. Santamaria, I. Rosa-Diaz, I. garcia, S. Dixit, S. Vallejos, C. Gotor, M. Martinez, V. Grbic, I. Diaz, Hydroxynitrile lyase defends Arabidopsis against *Tetranychus urticae*, Plant Physiol. 189 (2022) 2244–2258, https://doi.org/10.1093/plphys/kiac170.
[19] I. Rosa-Diaz, M.E. Santamaria, J.M. Acien, I. Diaz, Jasmonic acid catabolism in Arabidopsis defence against mites, Plant Sci. 334 (2023), 111784, https://doi.org/10.1016/j.plantsci.2023.111784.
[20] Y. Tada, S.H. Spoel, K. Pajerowska-Mukhtar, Z. Mou, J. Song, C. Wang, J. Zuo, X. Dong, Plant immunity requires conformational changes of NPR1 via S-nitrosylation and thioredoxins, Science 321 (2008) 952–956.
[21] M. Kinkema, W. Fan, X. Dong, Nuclear localization of NPR1 is required for activation of PR gene expression, Plant Cell 12 (2000) 2339–2350.
[22] J. Lorang, T. Kidarsa, C.S. Bradford, B. Gilbert, M. Curtis, S.C. Tzeng, C.S. Maier, T. J. Wolpert, Tricking the guard: exploiting plant defense for disease susceptibility, Science 338 (2012) 659–662.
[23] T.A. Sweat, T.J. Wolpert, Thioredoxin h5 is required for victorin sensitivity mediated by a CC-NBS-LRR gene in Arabidopsis, Plant Cell 19 (2007) 673–687.
[24] G.Z. Wu, E.H. Meyer, A.S. Richter, M. Schuster, Q. Ling, M.A. Schöttler, D. Walther, R. Zoschke, B. Grimm, R.P. Jarvis, et al., Control of retrograde signalling by protein import and cytosolic folding stress, Nat. Plants 5 (2019) 525–538.
[25] T. Nakagawa, T. Suzuki, S. Murata, S. Nakamura, T. Hino, K. Maeo, R. Tabata, T. Kawai, K. Tanaka, Y. Niwa, et al., Improved Gateway binary vectors: high-performance vectors for creation of fusion constructs in transgenic analysis of plants, Biosci. Biotechnol. Biochem. 71 (2007) 2095–2100.
[26] M. Seki, P. Carninci, Y. Nishiyama, Y. Hayashizaki, K. Shinozaki, High-efficiency cloning of Arabidopsis full-length cDNA by biotinylated CAP trapper, Plant J. 15 (1998) 707–720.
[27] M. Seki, M. Narusaka, A. Kamiya, J. Ishida, M. Satou, T. Sakurai, M. Nakajima, A. Enju, K. Akiyama, Y. Oono, et al., Functional annotation of a full-length Arabidopsis cDNA collection, Science 296 (2002) 141–145.
[28] S.J. Clough, A.F. Bent, Floral dip: a simplified method for Agrobacterium-mediated transformation of *Arabidopsis thaliana*, Plant J. 16 (1998) 735–743.
[29] J. Sambrook, D.W. Russell, Molecular Cloning: A Laboratory Manual, Cold Spring Harbor Laboratory Press, Cold Spring Harbor, N.Y, 2001.

[30] L. Oñate-Sánchez, J. Vicente-Carbajosa, DNA-free RNA isolation protocols for *Arabidopsis thaliana*, including seeds and siliques, BMC Res. Notes 1 (2008) 93.
[31] K.J. Livak, T.D. Schmittgen, Analysis of relative gene expression data using real-time quantitative PCR and the 2(-Delta Delta C(T)) method, Methods 25 (2001) 402–408.
[32] R. Oughtred, C. Stark, B.J. Breitkreutz, J. Rust, L. Boucher, C. Chang, N. Kolas, L. O'Donnell, G. Leung, R. McAdam, et al., The BioGRID interaction database: 2019 update, Nucleic Acids Res. 47 (D1) (2019) D529–D541.
[33] G. Bindea, B. Mlecnik, H. Hackl, P. Charoentong, M. Tosolini, A. Kirilovsky, W. H. Fridman, F. Pagès, Z. Trajanoski, J. Galon, ClueGO: a Cytoscape plug-in to decipher functionally grouped gene ontology and pathway annotation networks, Bioinformatics 25 (2009) 1091–1093.
[34] P.T. Shannon, M. Grimes, B. Kutlu, J.J. Bot, D.J. Galas, RCytoscape: tools for exploratory network analysis, BMC Bioinf. 14 (2013) 217.
[35] J.M. Shockey, S.K. Gidda, D.C. Chapital, J.C. Kuan, P.K. Dhanoa, J.M. Bland, S. J. Rothstein, R.T. Mullen, J.M. Dyer, Tung tree DGAT1 and DGAT2 have nonredundant functions in triacylglycerol biosynthesis and are localized to different subdomains of the endoplasmic reticulum, Plant Cell 18 (2006) 2294–2313.
[36] I. Diaz, M. Martinez, I. Isabel-LaMoneda, I. Rubio-Somoza, P. Carbonero, The DOF protein, SAD, interacts with GAMYB in plant nuclei and activates transcription of endosperm-specific genes during barley seed development, Plant J. 42 (2005) 652–662.
[37] A. Muñoz, M.M. Castellano, Coimmunoprecipitation of interacting proteins in plants, Methods Mol. Biol. 1794 (2018) 279–287.
[38] M.M. Bradford, A rapid and sensitive method for the quantitation of microgram quantities of protein utilizing the principle of protein-dye binding, Anal. Biochem. 72 (1976) 248–254.
[39] M. Cazaux, M. Navarro, K.A. Bruinsma, V. Zhurov, T. Negrave, T. Van Leeuwen, V. Grbic, M. Grbic, Application of two-spotted spider mite *Tetranychus urticae* for plant-pest interaction studies, J. Vis. Exp. 89 (2014), 51738.
[40] L.C. Terrón-Camero, E. Molina-Moya, M. Sanz-Fernández, L.M. Sandalio, M. C. Romero-Puertas, Detection of reactive oxygen and nitrogen species (ROS/RNS) during hypersensitive cell death, Methods Mol. Biol. 1743 (2018) 97–105.
[41] O. Martinez de Ilarduya, Q. Xie, I. Kaloshian, Aphid-induced defense responses in Mi-1-mediated compatible and incompatible tomato interactions, Mol. Plant Microbe Interact. 16 (2003) 699–708.
[42] J.J. Rodriguez-Herva, P. Gonzalez-Melendi, R. Cuartas-Lanza, M. Antunez-Lamas, I. Rio-Alvarez, Z. Li, et al., A bacterial cysteine protease effector protein interferes with photosynthesis to suppress plant innate immune responses, Cell Microbiol. 14 (2012) 669–681.
[43] M.C. Romero-Puertas, N. Campostrini, A. Mattè, P.G. Righetti, M. Perazzolli, L. Zolla, P. Roepstorff, M. Delledonne, Proteomic analysis of S-nitrosylated proteins in *Arabidopsis thaliana* undergoing hypersensitive response, Proteomics 8 (2008) 1459–1469.
[44] A.P. Ortega-Galisteo, M. Rodríguez-Serrano, D.M. Pazmiño, D.K. Gupta, L. M. Sandalio, M.C. Romero-Puertas, *S*-Nitrosylated proteins in pea (*Pisum sativum* L.) leaf peroxisomes: changes under abiotic stress, J. Exp. Bot. 63 (2012) 2089–2103.
[45] A. Durgbanshi, V. Arbona, O. Pozo, O. Miersch, J.V. Sancho, A. Gómez-Cadenas, Simultaneous determination of multiple phytohormones in plant extracts by liquid chromatography-electrospray tandem mass spectrometry, J. Agric. Food Chem. 53 (2005) 8437–8442.
[46] D. Yamazaki, K. Motohashi, T. Kasama, Y. Hara, T. Hisabori, Target proteins of the cytosolic thioredoxin in *Arabidopsis thaliana*, Plant Cell Physiol. 45 (2004) 18–27.
[47] A. Arnaiz, M. Martinez, P. Gonzalez-Melendi, V. Grbic, I. Diaz, M.E. Santamaria, Plant defenses against pests driven by a bidirectional promoter, Front. Plant Sci. 10 (2019) 930.
[48] S. Kneeshaw, S. Gelineau, Y. Tada, G.J. Loake, S.H. Spoel, Selective protein denitrosylation activity of Thioredoxin-h5 modulates plant Immunity, Mol. Cell 56 (2014) 153–162.
[49] C. Laloi, D. Mestres-Ortega, Y. Marco, Y. Meyer, J.P. Reichheld, The Arabidopsis cytosolic thioredoxin h5 gene induction by oxidative stress and its W-box-mediated response to pathogen elicitor, Plant Physiol. 134 (2004) 1006–1016.
[50] C. Belin, T. Bashandy, J. Cela, V. Delorme-Hinoux, C. Riondet, J.P. Reichheld, A comprehensive study of thiol reduction gene expression under stress conditions in *Arabidopsis thaliana*, Plant Cell Environ. 38 (2015) 299–314.
[51] A. Garcia, M.E. Santamaria, I. Diaz, M. Martinez, Disentangling transcriptional responses in plant defense against arthropod herbivores, Sci. Rep. 11 (2021), 12996.
[52] G. Noctor, J.P. Reichheld, C.H. Foyer, ROS-related redox regulation and signaling in plants, Semin. Cell Dev. Biol. 80 (2017) 3–12.
[53] C.T. Stomberski, D.T. Hess, J.S. Stamler, Protein S-nitrosylation: determinants of specificity and enzymatic regulation of S-nitrosothiol-based signaling, Antioxidants Redox Signal. 30 (2019) 1331–1351.
[54] J.L. Turrion-Gomez, E.P. Benito, Flux of nitric oxide between the necrotrophic pathogen Botrytis cinerea and the host plant, Mol. Plant Pathol. 12 (2011) 606–616.
[55] A. Baxter, R. Mittler, N. Suzuki, ROS as key players in plant stress signalling, J. Exp. Bot. 65 (2014) 1229–1240.
[56] S.-C. Park, Y.J. Jung, I.R. Kim, Y. Lee, Y.-M. Kim, M.-K. Jang, J.R. Lee, Functional characterization of thioredoxin h type 5 with antimicrobial activity from *Arabidopsis thaliana*, Biotechnol. Bioproc. Eng. 22 (2017) 129–135.
[57] L.A. Mur, E. Prats, S. Pierre, M.A. Hall, K.H. Hebelstrup, Integrating nitric oxide into salicylic acid and jasmonic acid/ethylene plant defense pathways, Front. Plant Sci. 4 (2013) 215.
[58] M.E. Santamaria, A. Garcia, A. Arnaiz, I. Rosa-Diaz, G. Romero-Hernandez, I. Diaz, M. Martinez, Comparative transcriptomics reveals hidden issues in the plant response to arthropod herbivores, J. Integr. Plant Biol. 32 (2021) 312–326.
[59] L.M. Sandalio, C. Gotor, L.C. Romero, M.C. Romero-Puertas, Multilevel regulation of peroxisomal proteome by post-translational modifications, Int. J. Mol. Sci. 20 (2019) 4881.
[60] L. Frungillo, M.J. Skelly, G.J. Loake, S.H. Spoel, I. Salgado, S-nitrosothiols regulate nitric oxide production and storage in plants through the nitrogen assimilation pathway, Nat. Commun. 5 (2014) 5401.
[61] A. Costa-Broseta, M. Castillo, J. León, Translational modifications of nitrate reductases autoregulates nitric ooxide biosynthesis in Arabidopsis, Int. J. Mol. Sci. 22 (2021) 549.
[62] C.M.J. Pieterse, S.C.M. van Wees, J.A. van Pelt, M. Knoester, R. Laan, H. Gerrits, P. J. Weisbeek, L.C. van Loon, A novel signaling pathway controlling induced systemic resistance in Arabidopsis, Plant Cell 10 (1998) 1571–1580.
[63] S.H. Spoel, A. Kpprnneef, S.M.C. Claessens, J.P. Korzelius, J.A. van Pelt, M. J. Mueller, A.J. Buchala, J.-P. Metraux, R. Brown, K. Kazan, et al., NPR1 modulates cross-talk between salicylate- and jasmonate-dependent defense pathways through a novel function in the cytosol, Plant Cell 15 (2003) 760–770.
[64] S.H. Spoel, Signal transduction in systemic immunity, Plant Cell 31 (2019) 1412–1413.
[65] P.L. Liu, L. Du, Y. Huang, S.M. Gao, M. Yu, Origin and diversification of leucine-rich repeat receptor-like protein kinase (LRR-RLK) genes in plants, BMC Evol. Biol. 17 (2017) 47.
[66] X. Ma, G. Xu, P. He, L. Shan, SERKing coreceptors for receptors, Trends Plant Sci. 21 (2016) 1017–1033.
[67] B. Li, M.A. Ferreira, M. Huang, L.F. Camargos, X. Yu, R.M. Teixeira, P.A. Carpinetti, G.C. Mendes, B.C. Gouveia-Mageste, C. Liu, et al., The receptor-like kinase NIK1 targets FLS2/BAK1 immune complex and inversely modulates antiviral and antibacterial immunity, Nat. Commun. 10 (2019) 4996.
[68] E. Smakowska-Luzan, G.A. Mott, K. Parys, M. Stegmann, T.C. Howton, M. Layeghifard, J. Neuhold, A. Lehner, J. Kong, K. Grünwald, et al., An extracellular network of Arabidopsis leucine-rich repeat receptor kinases, Nature 553 (2018) 342–346.
[69] S. Hou, X. Wang, D. Chen, X. Yang, M. Wang, D. Turrà, A. Di Pietro, W. Zhang, The secreted peptide PIP1 amplifies immunity through receptor-like kinase 7, PLoS Pathog. 10 (2014), e1004331.
[70] N. Yuan, S. Yuan, Z. Li, M. Zhou, P. Wu, Q. Hu, V. Mendu, L. Wang, H. Luo, STRESS INDUCED FACTOR 2, a leucine-rich repeat kinase regulates basal plant pathogen defense, Plant Physiol. 176 (2018) 3062–3080.
[71] Y. Xue, Z. Liu, X. Gao, C. Jin, L. Wen, X. Yao, J. Ren, GPS-SNO: computational prediction of protein S-nitrosylation sites with a modified GPS algorithm, PLoS One 5 (2010), e11290.
[72] H.-L. Zhou, C.T. Stomberski, J.S. Stamler, Cross talk between *S*-Nitrosylation and Phosphorylation involving kinases and nitrosylases, Circ. Res. 122 (2018) 1485–1487.